

Diagonal and off-diagonal quark number susceptibilities at high temperatures

H.-T. Ding,¹ Swagato Mukherjee,² H. Ohno,^{2,3} P. Petreczky,² and H.-P. Schadler^{2,4}

¹*Key Laboratory of Quark & Lepton Physics (MOE) and Institute of Particle Physics, Central China Normal University, Wuhan, 430079, China*

²*Physics Department, Brookhaven National Laboratory, Upton, NY 11973, USA*

³*Center for Computational Sciences, University of Tsukuba, Tsukuba, Ibaraki 305-8577, Japan*

⁴*Institute of Physics, University of Graz, 8010 Graz, Austria*

We present continuum extrapolated lattice QCD results for up to fourth-order diagonal and off-diagonal quark number susceptibilities in the high temperature region of 300 – 700 MeV. Lattice QCD calculations are performed using 2+1 flavors of highly improved staggered quarks with nearly physical quark masses and at four different lattice spacings. Comparisons of our results with recent weak coupling calculations yield reasonably good agreements for the entire temperature range.

I. INTRODUCTION

At high temperatures strongly interacting matter undergoes a deconfinement transition, where thermodynamics can be described in terms of quarks and gluons [1–3]. Lattice QCD studies [1–3] as well as results from heavy-ion collision experiments [4] suggest that at least up to temperatures couple of times larger than the transition temperature quark-gluon plasma (QGP) may behave as a strongly coupled liquid. The asymptotic freedom of QCD guarantees that at sufficiently high temperatures QGP becomes weakly coupled and should be described by weak coupling expansion results. However, nonperturbative effects could still remain important even at very high temperatures due to the infrared problems arising from the chromomagnetic sector [5]. Thus, quantitative validations of weak coupling QCD calculations against fully nonperturbative lattice QCD results are necessary to ascertain the temperature range where the strongly coupled QGP liquid goes over to a weakly coupled quark-gluon gas.

Fluctuations of and correlations among the conserved charges are known to be sensitive probes of deconfinement and are also suitable for testing the weakly or strongly coupled nature of QGP. The study of fluctuations and correlations of conserved charges on the lattice was initiated some time ago [6–9]. At low temperature fluctuations and correlations of conserved charges can be understood in terms of an uncorrelated hadron gas [10–17]. Deconfinement is signaled by a sudden breakdown of such a hadronic description in the vicinity of the QCD transition temperature [12, 16].

Fluctuations of and correlations among the conserved charges are defined through the appropriate derivatives of the pressure, p with respect to the chemical potentials associated with the corresponding conserved charges. In 2+1 flavor QCD there are three chemical potentials corresponding to baryon number, electric charge and strangeness. Since at high temperatures the relevant degrees of freedom are quarks and gluons, it is natural to use the flavor chemical potentials corresponding to the u (up), d (down) and s (strange) quark numbers instead of the three conserved charge chemical potentials. In the

flavor basis the fluctuations and correlations of charges get mapped into the diagonal (χ_n^q) and the off-diagonal ($\chi_{nm}^{qq'}$) quark number susceptibilities

$$\chi_n^q = \frac{\partial^n (p/T^4)}{\partial (\mu_q/T)^n}, \text{ and } \chi_{nm}^{qq'} = \frac{\partial^{n+m} (p/T^4)}{\partial (\mu_q/T)^n \partial (\mu_{q'}/T)^m}. \quad (1)$$

Here, μ_q and $\mu_{q'}$ are the chemical potentials corresponding to quark flavor q and q' , with $q, q' = u, d, s$, and n, m denote the number of derivatives taken with respect to the quark flavors.

At sufficiently high temperatures the diagonal and off-diagonal quark number susceptibilities should be described by weak coupling expansion results. Second-order quark number susceptibilities have been studied in weak coupling expansion for some time [18–21]. Recently also weak coupling results for the fourth-order fluctuations and correlations have been presented [22–27]. The validity of these weak coupling expansion results for the second-order diagonal susceptibilities χ_2^q has been tested against the accurate continuum extrapolated lattice QCD results in Ref. [28]. Here we extend this previous study to perform accurate continuum extrapolated lattice QCD calculations of fourth-order diagonal quark number susceptibility χ_4^q and subsequently compare them with weak coupling perturbative QCD results to validate the weak coupling regime of QGP. Diagrammatically, the off-diagonal quark number susceptibilities only consist of quark-line disconnected diagrams and corrections to the tree level generically start at higher orders of the coupling. Thus, these off-diagonal susceptibilities provide more stringent tests of the weak coupling regime of QGP. Our present study also includes lattice calculations and their comparisons with weak coupling results of up to fourth-order off-diagonal quark number susceptibilities.

The rest of the paper is organized as follows. In Sec. II we describe the details of our lattice QCD calculations. Sec. III is dedicated to the discussion of fourth order diagonal quark number susceptibilities, including the details of continuum extrapolations and comparison with weak coupling approaches. In Sec. IV we present our results for the off-diagonal quark number susceptibilities. Finally, Sec. V contains our conclusions.

II. DETAILS OF THE LATTICE SIMULATIONS

We performed lattice calculations in 2+1 flavor QCD using the highly improved staggered quark (HISQ) action [29]. Lattice sizes were chosen to be $N_\sigma^3 \times N_\tau$ with $N_\tau = 6, 8, 10$ and 12 and a fixed aspect ratio of $N_\sigma/N_\tau = 4$. The gauge configurations used in this study were generated by the HotQCD Collaboration using the physical value of the strange quark mass m_s and degenerate up and down quark masses $m_u = m_d = m_l = m_s/20$ [30, 31]. The latter corresponds to a pion mass of 161 MeV in the continuum limit [30]. For each value of N_τ the temperature was varied by varying the lattice spacing a or equivalently the lattice gauge coupling $\beta = 10/g^2$. The lattice spacing has been fixed using the r_1 scale defined in terms of the static quark potential

$$r^2 \frac{dV}{dr} \Big|_{r=r_1} = 1. \quad (2)$$

We used the parametrization of a/r_1 from Ref. [31]. As in Ref. [30] we use $r_1 = 0.3106$ fm to convert to physical units. To extend the temperature coverage in our calculations additional gauge configurations have been generated for $\beta = 10/g^2 = 8.0, 8.2$ and 8.4 on $32^3 \times 8, 40^3 \times 10$ and $48^3 \times 12$ lattices. As in Refs. [30, 31] we use the Rational Hybrid Monte Carlo algorithm [32]. About 2000–4000 gauge configurations separated by ten molecular dynamic trajectories of unit length have been generated for each value of the gauge coupling β . The complete list of the gauge configurations used in this study can be found in the Appendix.

The quark number susceptibilities can be expressed in terms of the quark matrix and its inverse, and the corresponding formulas were given in Refs. [8, 9, 33]. The necessary operators are evaluated using the random noise method with unbiased estimators (see Ref. [33] for details). We used between 150 to 250 random source vectors to evaluate the needed operators depending on the lattice volume and the value of β . We have found that this number of source vectors is sufficient to ensure that the noise due to gauge field fluctuations is larger than the noise from the stochastic estimators. In a few cases, some operators have been estimated with many more random source vectors to ensure that there are no additional systematic errors due to the limited number of source vectors. In the Appendix we give a detailed account for the number of random source vectors used in our study. The inversion of the quark matrix was performed in double precision, and the squared residual of the inversion was less than 10^{-19} .

III. DIAGONAL QUARK NUMBER SUSCEPTIBILITIES

In this section we will discuss our results on diagonal quark number susceptibilities. The second-order light

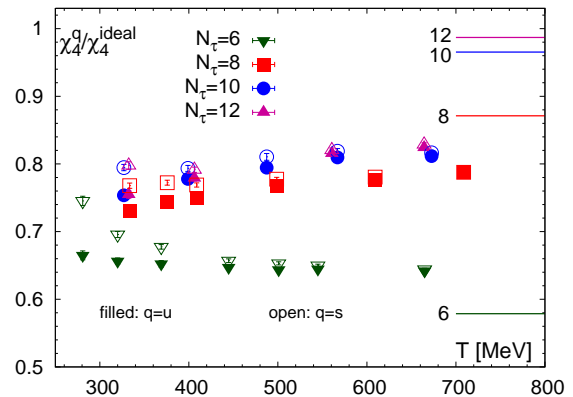


FIG. 1. The light ($q = u$) and strange ($q = s$) fourth-order quark number susceptibilities shown as filled and open symbols, respectively, for different values of the lattice temporal extent N_τ and normalized by the results for the continuum, massless ideal gas limit $\chi_4^{\text{ideal}} = 6/\pi^2$. The horizontal lines denote the lattice ideal gas results for different values of N_τ .

and strange quark number susceptibilities have been discussed in Ref. [28] in great detail using HISQ action, including the continuum extrapolation. Our results for the second-order quark number susceptibilities agree with the findings of Ref. [28], and therefore we will not discuss these further. In Fig. 1 we show our results for the light and strange fourth-order quark number susceptibilities χ_4^q ($q = u, s$) for $N_\tau = 6, 8, 10$ and 12 . The cutoff dependence of χ_4^q is similar to that of $\chi_2^{u,s}$; the continuum is approached from below as suggested by the cutoff effects in the lattice free theory. Similar to the case of χ_2^q [28], the size of the cutoff effects is smaller than in the free theory, cf. Fig. 1. The quark mass dependence is, however, opposite to the case of χ_2^q for $T < 500$ MeV. Namely, the fourth-order light quark number susceptibilities are below the strange quark number susceptibilities, while for the second-order susceptibilities $\chi_2^s < \chi_2^u$ [28]. For $T > 500$ MeV the quark mass effects in the fourth-order quark number susceptibilities are smaller than the statistical uncertainty.

To perform the continuum extrapolation, we first interpolate the lattice results as a function of the temperature using smoothing splines. The spline interpolation is performed using the R-package [34]. The errors of the spline are estimated using the bootstrap method. At selected values of the temperature in the interval of $T = 340$ MeV to $T = 660$ MeV, separated by 20 MeV, we performed continuum extrapolations using the interpolated values of χ_4^q and the corresponding bootstrap errors. Illustrative results for the continuum extrapolations for χ_4^q are shown in Fig. 2. For each temperature we performed the continuum extrapolation using the form motivated by the lattice free theory [35],

$$\chi_4^q(N_\tau) = a + b/N_\tau^4 + c/N_\tau^6. \quad (3)$$

We also performed extrapolations using only the data

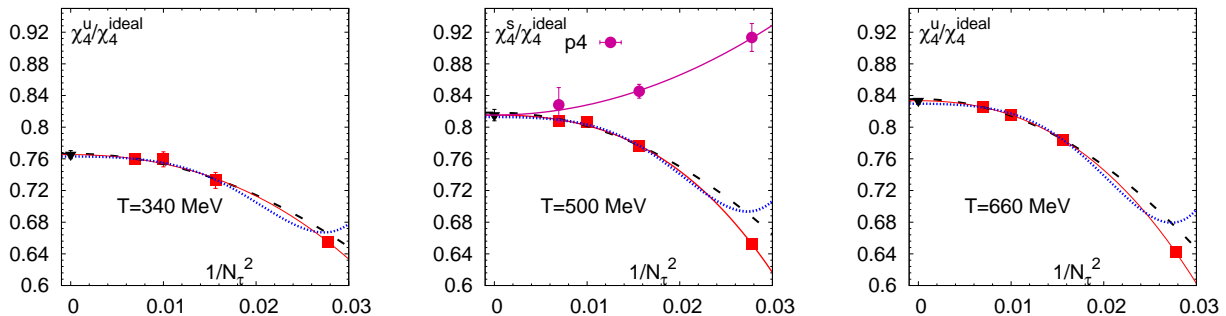


FIG. 2. Continuum extrapolations of χ_4^q at three representative temperatures. In the middle panel, we show extrapolation for χ_4^s and compare our results with the N_τ dependence of χ_4^s obtained with p4 action [28]. The solid and dashed lines correspond to continuum extrapolations using Eq. (3), while the dotted lines correspond to extrapolations performed using Eq. (4); see the main text. The filled triangle corresponds to the continuum value. All the results have been normalized by $\chi_4^{\text{ideal}} = 6/\pi^2$.

for $N_\tau \geq 8$ and setting $c = 0$. These extrapolations typically give larger continuum values but remain compatible within errors with the original extrapolations. These fits are shown as solid and dashed lines, respectively, in Fig. 2. We do not find evidence for a significant $1/N_\tau^2$ term in the cutoff dependence for χ_4^q . This is evident from the N_τ dependence of our results shown in Fig. 2. A similar situation was observed for χ_2^q [28]. Since the cutoff dependence of χ_4^q qualitatively follows the lattice free theory expectation we also performed continuum extrapolation using the form

$$\chi_4^q(N_\tau) = e + f \cdot (\chi_4^{q,\text{lat-ideal}}(N_\tau) - \chi_4^{\text{ideal}}), \quad (4)$$

where $\chi_4^{q,\text{lat-ideal}}(N_\tau)$ is the lattice free theory result and $\chi_4^{\text{ideal}} = 6/\pi^2$ is the continuum free theory result for the fourth-order quark number susceptibility. This simple two-parameter fit describes the data well. The results of these fits are also shown in Fig. 2 as dotted lines. For the coefficient f we get values ranging from about 0.30 at the lowest temperature to about 0.43 at the highest temperature; i.e., cutoff effects are only 30% – 40% of those in the free theory. The central values of the extrapolations obtained from Eq. (4) are typically smaller than the ones obtained from the three-parameter fit with Eq. (3), but still compatible within errors. In other words, there are no statistically significant deviations between the different continuum extrapolations. Therefore, the extrapolated values obtained from three-parameter fits with Eq. (3) will be used as our continuum results. Since the different continuum extrapolations give a difference of the order of the statistical errors, we conservatively estimate the total error on our continuum results for χ_4^q as twice the statistical error obtained from our three-parameter fits.

In Fig. 2 we also show the lattice results for χ_4^s for $T = 500$ MeV obtained with p4 action for $N_\tau = 6, 8$ and 12 [28]. As discussed in Ref. [28], the continuum limit for p4 action is approached from above, and the cutoff dependence in this case does not follow the free theory expectation; the leading-order cutoff dependence goes like

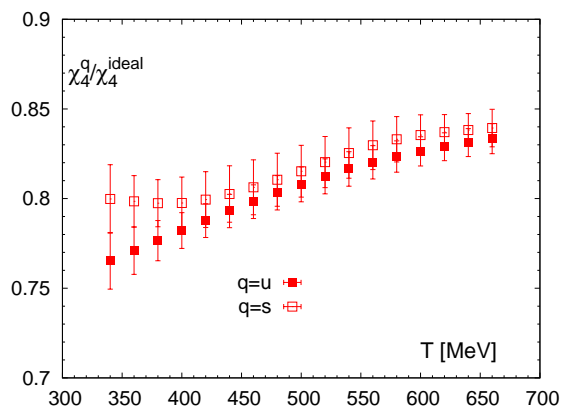


FIG. 3. The continuum extrapolated results for χ_4^u and χ_4^s normalized by the corresponding massless ideal gas value $\chi_4^{\text{ideal}} = 6/\pi^2$.

$1/N_\tau^2$. As was also discussed there, the quality of the p4 data does not allow a reliable continuum extrapolation for χ_4^s . However, in the continuum limit, the results obtained with HISQ action and p4 action should of course agree. Therefore, we fit the cutoff dependence of the p4 data using the form $a + g/N_\tau^2 + h/N_\tau^4$ and requiring that in the continuum limit it agrees with the HISQ result. This fit gives $\chi^2/\text{d.o.f.} \simeq 0.1$. Therefore, we can at least say that the p4 data are consistent with the continuum extrapolations performed with HISQ action. The continuum extrapolated results for χ_4^u and χ_4^s are shown in Fig. 3 as a function of the temperature. We can see that $\chi_4^s > \chi_4^u$ but the difference between χ_4^s and χ_4^u becomes smaller with increasing temperature. The continuum extrapolated results for χ_4^q are provided in Table I.

The deviation of χ_4^q from the ideal gas limit at the highest temperature studied by us is 15%. This should be compared to the continuum result for χ_2^q which is only 6% below the ideal gas limit at a similar temperature [28]. It is interesting to see whether these deviations from the ideal gas limit can be understood in terms of weak cou-

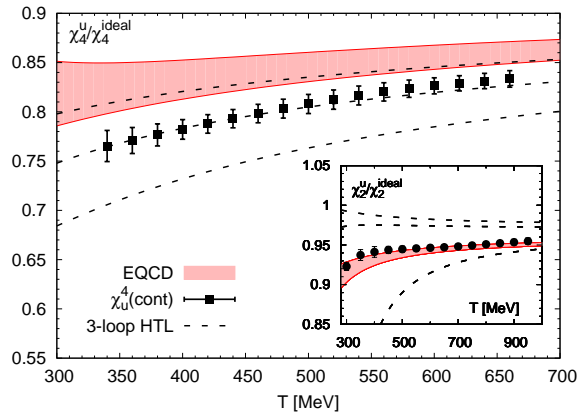


FIG. 4. The continuum extrapolated result for χ_4^u compared to perturbative EQCD calculations shown as the shaded band. The width of the band corresponds to the variation of the renormalization scale from πT to $4\pi T$. The dashed lines correspond to the three-loop HTL calculations evaluated for the renormalization scale $\Lambda = 4\pi T$, $2\pi T$ and πT (from top to bottom). All results have been normalized by the corresponding massless ideal gas results of $\chi_4^{\text{ideal}} = 6/\pi^2$. The inset shows the comparison of the lattice and weak coupling calculations for χ_2^u [28] normalized by $\chi_2^{\text{ideal}} = 1$.

pling expansions. The fourth order quark number susceptibilities have been calculated in three-loop hard thermal loop (HTL) perturbation theory recently in Ref. [27] and in perturbative calculations using dimensionally reduced electrostatic QCD (EQCD) [24]. These weak coupling results are compared with our continuum results for χ_4^u in Fig. 4. We show the scale uncertainty of the perturbative results by varying the renormalization scale Λ from πT to $4\pi T$. The comparison of the continuum lattice results for χ_2^u [28] with weak coupling calculations is also shown in Fig. 4 as an inset. The EQCD band is above the continuum extrapolated lattice data for χ_4^u , while these calculations give results for χ_2^u that agree with the lattice data. So there remains some tension between the EQCD calculations and the lattice results on second and fourth-order quark number susceptibilities. The three-loop HTL perturbative result agrees very well with our lattice data for the renormalization scale $\Lambda = 2\pi T$. This scale choice, however, overpredicts the value of χ_2^u . Although the scale uncertainty in the three-loop HTL calculation of χ_2^u is rather large, it should be noted that, once the renormalization scale Λ is fixed by comparing one observable with the corresponding lattice QCD result all the other quantities are completely parameter-free predictions of HTL calculations without any uncertainty. Unfortunately, the lattice QCD results for χ_2^q and χ_4^q cannot be simultaneously reproduced by the three-loop HTL calculations with a single renormalization scale for the coupling. Overall the three-loop HTL perturbative results agree with the lattice data within a somewhat large scale uncertainty.

IV. OFF-DIAGONAL QUARK NUMBER SUSCEPTIBILITIES

In this section we show our results on off-diagonal quark number susceptibilities and compare them with weak coupling calculations. The off-diagonal susceptibilities vanish in the infinite temperature limit, i.e., for the ideal quark gas. In fact, using weak coupling calculations, one can show that they are related to the coupling of quarks to soft (static) gluons. In the language of EQCD, one may say that they do not receive contribution from the scale $2\pi T$. In particular, the leading-order contribution to $\chi_{22}^{qq'}$ comes from the term proportional to Tm_D^3 (the so-called plasmon term) in the expression of the pressure, with m_D being the leading-order Debye mass. Thus, the leading-order contribution to $\chi_{22}^{qq'}$ is of order $g^3 \sim \alpha_s^{3/2}$. The leading-order contribution to $\chi_{11}^{qq'}$ is order $g^6 \sim \alpha_s^3$ and is sensitive to the static chromomagnetic sector. Therefore, it is nonperturbative and can only be calculated using lattice simulations of EQCD [21]. Since the off-diagonal quark number susceptibilities at high temperature are mostly sensitive to soft gluon fields, the cutoff (N_τ) dependence of these quantities in lattice calculations using HISQ is expected to be small at high temperatures. Our lattice QCD results for χ_{11}^{ud} and χ_{22}^{us} are shown in Fig. 5. As expected, the apparent cutoff dependence of the off-diagonal quark susceptibilities is considerably smaller than for the diagonal ones. The off-diagonal susceptibilities are small, which is in qualitative agreement with weak coupling expectations discussed above. Since the cutoff dependence of the off-diagonal susceptibilities is quite small, it is possible to perform a comparison with weak coupling calculations using the lattice data at fixed N_τ . Nevertheless, we performed continuum extrapolations also for off-diagonal quark number susceptibilities. The procedure of continuum extrapolation here is similar to that for diagonal quark number susceptibilities. We first perform an interpolation in the temperature and then continuum extrapolations at the same temperature values as before separated by 20 MeV. We performed continuum extrapolations fitting the N_τ dependence of the lattice data with $a + b/N_\tau^2 + c/N_\tau^4$. We also performed fits using only $N_\tau \geq 8$ data and setting $c = 0$. Both fits give result that agree well within the errors. In the case of χ_{22}^{us} it was also possible to set $b = 0$, i.e., perform fits to a constant for $N_\tau \geq 8$. These fits give the result with the smallest errors but are consistent with the above fits. In the case of χ_{11}^{ud} , we performed fits with $c = 0$ to obtain the continuum estimate. In addition averaging over $N_\tau = 10$ and $N_\tau = 12$ data for χ_{11}^{ud} gave results which are consistent with the above continuum estimate. We used the two-parameter fits and the corresponding errors for our final continuum estimates for χ_{22}^{ud} and χ_{11}^{ud} .

These continuum estimates are also shown in Fig. 5. The numerical values of the continuum extrapolated off-diagonal susceptibilities are also presented in Table I. We

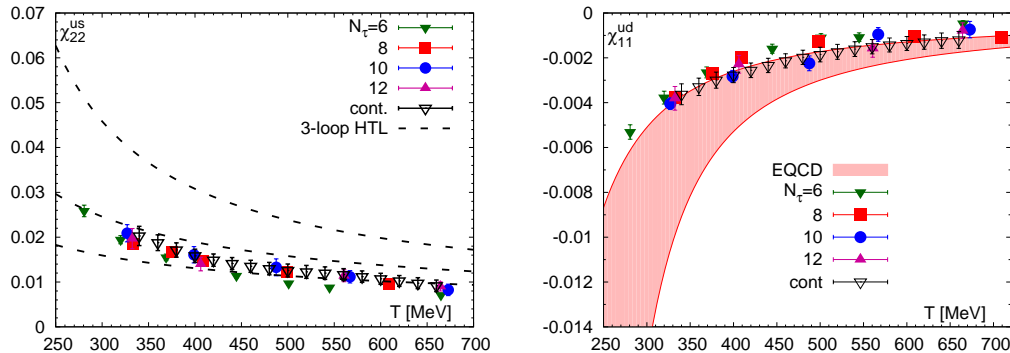


FIG. 5. The fourth-order off-diagonal susceptibility χ_{22}^{us} (left) and the second order off-diagonal quark number susceptibility χ_{11}^{ud} (right) calculated for different values of N_τ . The lattice results are compared to EQCD calculations [21] shown as the shaded band corresponding to renormalization scale variation from πT to $4\pi T$ and to three-loop HTL perturbation theory [27] shown with the dashed lines for renormalization scale $\Lambda = \pi T$, $2\pi T$ and $4\pi T$ (from top to bottom).

also calculated χ_{11}^{us} and χ_{22}^{ud} and found that within the estimated errors they agree with χ_{11}^{ud} and χ_{22}^{us} .

Now let us compare our lattice results with weak coupling calculations in more details. In Fig. 5 we also show the results from three-loop HTL perturbation theory for χ_{22}^{us} using three choices of the renormalization scale $\Lambda = \pi T$, $2\pi T$ and $4\pi T$ [27]. The scale choice $\Lambda = 4\pi T$ works best for the higher temperature, while for a lower temperature, the choice $\Lambda = 2\pi T$ seems to be better. Overall it is fair to say that, within the uncertainties, the lattice and the three-loop HTL perturbation theory results agree. We note that the three-loop HTL calculation for quark number susceptibilities has been performed in the limit of vanishing quark masses. As stated above the quark mass effects are negligible for $\chi_{22}^{qq'}$, and therefore comparison of three-loop HTL results and the lattice results for χ_{22}^{us} is justified. We compare our results for χ_{11}^{ud} with EQCD calculations of Ref. [21]. In EQCD χ_{11}^{ud} can be written as

$$\chi_{11}^{ud} = \frac{g_E^6}{\pi^3} \left(\frac{5}{288\pi^4} \ln(4y) + \frac{5}{48\pi^4} \beta_M + \delta\chi_3(y) \right), \quad (5)$$

where $y = m_E^2/g_E^4$, g_E and m_E are the gauge coupling and the mass parameter of EQCD which can be calculated at any order in perturbation theory [36]. The constant β_M is a nonperturbative constant that determines the leading-order contribution to χ_{11}^{ud} . We use the value $\beta_M = 0.1$ determined in Ref. [21]. The function $\delta\chi_3(y)$ parameterizes higher order corrections and was calculated in Ref. [21]. Using this as well as the next-to-leading-order expression for y from Ref. [37] together with the next-to-next-leading-order result for g_E [38], we calculate the EQCD result for χ_{11}^{ud} . This result is shown in Fig. 5 as a band. The width of the band for χ_{11}^{ud} shown in Fig. 5 corresponds to the error on $\delta\chi_3$ and the scale variation between $\Lambda = \pi T$ and $\Lambda = 4\pi T$ combined. We see that there is a fair agreement between the lattice results and the EQCD calculation for χ_{11}^{ud} .

We also calculated the three other fourth-order off-

diagonal quark number susceptibilities, χ_{31}^{ud} , χ_{31}^{us} and χ_{13}^{us} . Unfortunately, these quantities are very noisy, but within large errors appear to be both temperature independent as well as N_τ independent. If we fit all the available lattice data in the temperature range $T = 280 - 710$ MeV with a constant, we obtain the following estimates:

$$\chi_{31}^{ud} = 0.00020 \pm 0.00015, \quad (6)$$

$$\chi_{31}^{us} = 0.00071 \pm 0.00030, \quad (7)$$

$$\chi_{13}^{us} = 0.00060 \pm 0.00030. \quad (8)$$

We see that these off-diagonal susceptibilities are similar in magnitude to χ_{11}^{ud} which may be expected in the weak coupling calculations.

V. CONCLUSIONS

In this paper we have extended the study of lattice QCD calculations quark number susceptibilities at high temperatures using the HISQ action to include fourth-order diagonal as well as off-diagonal quark number susceptibilities. In our calculations we use lattices with temporal extent $N_\tau = 6, 8, 10$ and 12 , and we cover temperatures ranging from 300 up to 700 MeV. We have obtained sufficiently accurate reliable continuum extrapolated lattice QCD results at high enough temperatures to perform meaningful comparisons with weak coupling QCD calculations. We find that the cutoff dependence of the fourth-order diagonal quark number susceptibilities χ_4^q is similar to the cutoff dependence of the second order quark number susceptibility χ_2^q [28], and continuum extrapolations can be performed in a similar manner. The systematic errors of the continuum extrapolations are quite small, smaller than or equal to the statistical errors. We compared our continuum extrapolated results for χ_4^u to three-loop HTL perturbation theory as well as to EQCD results. The result of three-loop HTL perturbation theory agrees very well with our continuum extrapolated result for χ_4^u . However, three-loop HTL calcula-

tions cannot simultaneously reproduce the lattice QCD results for χ_2^q and χ_4^q with the same choice of the renormalization scale for the coupling. The EQCD result of Ref. [24] for χ_4^u is somewhat above our continuum lattice result, while it agrees with the continuum lattice results for χ_2^u [28].

In the case of the off-diagonal susceptibilities, we also find decent agreements between the lattice and the weak coupling results for χ_{11}^{ud} and χ_{22}^{ud} . From our analysis it is clear that lattice results provide stringent tests for different weak coupling approaches at high temperatures. The agreement between the lattice and the weak coupling results suggests that for $T > 300$ MeV quark degrees of freedom are weakly coupled.

While this paper was being finalized, Ref. [39] appeared. Reference [39] performed similar lattice QCD calculations with a different fermionic discretization scheme and compared up to fourth-order diagonal and off-diagonal susceptibilities with the weak coupling results. The lattice results and hence the conclusions of Ref. [39] is very similar to our present study.

ACKNOWLEDGMENTS

This work was supported by U.S. Department of Energy under Contract No. DE-SC0012704. H.-P. Schadler was funded by the FWF DK W1203, ‘‘Hadrons in Vacuum, Nuclei and Stars’’. The authors thank F. Karsch and P. Steinbrecher for interesting discussions. The numerical computations have been carried out on the clusters of USQCD collaboration, on the BlueGene supercomputers at the New York Center for Computational Sciences (NYCCS) and on Vienna Scientific Cluster (VSC). The calculations have been performed using the publicly available MILC code. We thank S. Mogliacci and N. Haque for sending the numerical values of their calculations.

Appendix: Details of lattice calculations

In this Appendix we present some details of our calculations. In Tables II, III, IV and V we show the gauge coupling $\beta = 10/g^2$ and the corresponding temperatures for different lattice sizes. The number of gauge configurations used in the analysis is shown as the last column of the tables. We estimate the fermion operators involving light (u or d) quarks using $N_{sv,l}$ random source vectors, while for the operators involving strange quarks we use $N_{sv,s}$ source vectors. We tried to improve the stochastic estimates by using additional source vectors for all operators that only require two inversions. In most cases these operators turn out to be the noisiest but because of fewer inversions are cheaper to calculate. The number of additional source vectors is denoted by $N_{sv,l}^{imp}$ and $N_{sv,s}^{imp}$ for light and strange quark operators, respectively.

TABLE I. The continuum estimates for the diagonal and off-diagonal quark number susceptibilities.

T [MeV]	χ_4^u	χ_4^s	$\chi_{11}^{ud} \cdot 10^3$	χ_{22}^{ud}
340	0.4653(48)	0.4862(58)	-3.62(46)	0.0203(21)
360	0.4687(41)	0.4854(43)	-3.29(39)	0.0188(18)
380	0.4721(34)	0.4848(40)	-2.99(36)	0.0171(16)
400	0.4755(30)	0.4849(44)	-2.77(33)	0.0158(15)
420	0.4789(29)	0.4860(47)	-2.56(33)	0.0149(14)
440	0.4821(28)	0.4879(47)	-2.34(32)	0.0141(13)
460	0.4853(29)	0.4902(47)	-2.13(31)	0.0135(13)
480	0.4883(29)	0.4927(45)	-1.98(32)	0.0130(14)
500	0.4912(30)	0.4956(44)	-1.85(33)	0.0126(14)
520	0.4939(30)	0.4987(43)	-1.73(33)	0.0123(14)
540	0.4964(29)	0.5018(43)	-1.61(33)	0.0120(14)
560	0.4986(28)	0.5044(41)	-1.50(32)	0.0117(13)
580	0.5006(27)	0.5065(38)	-1.42(31)	0.0112(17)
600	0.5023(25)	0.5079(34)	-1.36(31)	0.0107(12)
620	0.5039(24)	0.5089(30)	-1.30(32)	0.0102(12)
640	0.5053(24)	0.5096(28)	-1.24(34)	0.0097(12)
660	0.5067(26)	0.5103(32)	-1.20(38)	0.0091(13)

For some ensembles we used many more source vectors to check for systematic errors.

TABLE II. Parameters of the calculations for $24^3 \times 6$ lattices

β	T (MeV)	$N_{sv,l}$	$N_{sv,l}^{imp}$	$N_{sv,s}$	$N_{sv,s}^{imp}$	# configurations
6.664	281.1	150	0	150	0	2990
6.800	320.5	150	0	150	0	3000
6.950	369.8	150	0	150	0	3000
7.150	445.9	150	0	150	0	2540
7.280	502.5	150	0	150	0	2720
7.373	546.7	150	0	150	0	2310
7.596	667.2	150	0	150	0	3000

TABLE III. Parameters of the calculations for $32^3 \times 8$ lattices

β	T (MeV)	$N_{sv,l}$	$N_{sv,l}^{imp}$	$N_{sv,s}$	$N_{sv,s}^{imp}$	# configurations
7.150	334.4	250	0	250	0	4020
7.280	376.8	250	0	250	0	4080
7.373	410.0	250	1000	250	0	3940
7.596	500.4	250	0	250	0	4050
7.825	611.5	250	0	250	0	3920
8.000	711.3	250	0	250	0	1800

TABLE IV. Parameters of the calculations for $40^3 \times 10$ lattices

β	T (MeV)	$N_{sv,l}$	$N_{sv,l}^{imp}$	$N_{sv,s}$	$N_{sv,s}^{imp}$	# configurations
7.373	328.0	300	0	300	0	4060
7.596	400.3	300	0	300	0	3180
7.825	489.2	300	0	300	0	3090
8.000	569.1	600	600	200	0	2670
8.200	675.3	200	0	200	0	1590

TABLE V. Parameters of the calculations for $48^3 \times 12$ lattices

β	T (MeV)	$N_{sv,l}$	$N_{sv,l}^{imp}$	$N_{sv,s}$	$N_{sv,s}^{imp}$	# configurations
7.596	333.6	250	250	250	250	3360
7.825	407.7	250	250	250	250	3020
8.200	562.7	250	250	250	250	2740
8.400	666.9	250	250	250	250	2710

- [1] P. Petreczky, J. Phys. G **39**, 093002 (2012), arXiv:1203.5320 [hep-lat].
- [2] O. Philipsen, Prog. Part. Nucl. Phys. **70**, 55 (2013), arXiv:1207.5999 [hep-lat].
- [3] H.-T. Ding, F. Karsch, and S. Mukherjee, (2015), arXiv:1504.05274 [hep-lat].
- [4] B. Muller and J. L. Nagle, Ann. Rev. Nucl. Part. Sci. **56**, 93 (2006).
- [5] A. D. Linde, Phys. Lett. B **96**, 289 (1980).
- [6] R. V. Gavai and S. Gupta, Phys. Rev. D **67**, 034501 (2003), arXiv:hep-lat/0211015 [hep-lat].
- [7] C. Bernard *et al.* (MILC Collaboration), Phys. Rev. D **71**, 034504 (2005), arXiv:hep-lat/0405029 [hep-lat].
- [8] C. Allton *et al.*, Phys. Rev. D **68**, 014507 (2003), arXiv:hep-lat/0305007 [hep-lat].
- [9] C. Allton *et al.*, Phys. Rev. D **71**, 054508 (2005), arXiv:hep-lat/0501030 [hep-lat].
- [10] M. Cheng *et al.*, Phys. Rev. D **79**, 074505 (2009), arXiv:0811.1006 [hep-lat].
- [11] A. Bazavov *et al.*, Phys. Rev. Lett. **109**, 192302 (2012), arXiv:1208.1220 [hep-lat].
- [12] A. Bazavov *et al.*, Phys. Rev. Lett. **111**, 082301 (2013), arXiv:1304.7220 [hep-lat].
- [13] R. Bellwied, S. Borsanyi, Z. Fodor, S. D. Katz, and C. Ratti, Phys. Rev. Lett. **111**, 202302 (2013), arXiv:1305.6297 [hep-lat].
- [14] S. Borsanyi *et al.*, Phys. Rev. Lett. **111**, 062005 (2013), arXiv:1305.5161 [hep-lat].
- [15] A. Bazavov *et al.*, Phys. Rev. Lett. **113**, 072001 (2014), arXiv:1404.6511 [hep-lat].
- [16] A. Bazavov *et al.*, Phys. Lett. B **737**, 210 (2014), arXiv:1404.4043 [hep-lat].
- [17] C. Gattringer and H.-P. Schadler, Phys. Rev. D **91**, 074511 (2015), arXiv:1411.5133 [hep-lat].
- [18] J. Blaizot, E. Iancu, and A. Rebhan, Phys. Lett. B **523**, 143 (2001), arXiv:hep-ph/0110369 [hep-ph].
- [19] A. Vuorinen, Phys. Rev. D **67**, 074032 (2003), arXiv:hep-ph/0212283 [hep-ph].
- [20] A. Rebhan, *Strong and Electroweak Matter 2002* (World Scientific, 2003) arXiv:hep-ph/0301130 [hep-ph].
- [21] A. Hietanen and K. Rummukainen, J. High Energy Phys. **04**, 078 (2008), arXiv:0802.3979 [hep-lat].
- [22] N. Haque and M. G. Mustafa, arXiv:1007.2076 [hep-ph].
- [23] J. O. Andersen, S. Mogliacci, N. Su, and A. Vuorinen, Phys. Rev. D **87**, 074003 (2013), arXiv:1210.0912 [hep-ph].
- [24] S. Mogliacci, J. O. Andersen, M. Strickland, N. Su, and A. Vuorinen, Journal of High Energy Phys. **12**, 055 (2013), arXiv:1307.8098 [hep-ph].
- [25] N. Haque, M. G. Mustafa, and M. Strickland, Journal of High Energy Phys. **07**, 184 (2013), arXiv:1302.3228 [hep-ph].
- [26] N. Haque, J. O. Andersen, M. G. Mustafa, M. Strickland, and N. Su, Phys. Rev. D **89**, 061701 (2014), arXiv:1309.3968 [hep-ph].
- [27] N. Haque, A. Bandyopadhyay, J. O. Andersen, M. G. Mustafa, M. Strickland, *et al.*, Journal of High Energy Phys. **05**, 027 (2014), arXiv:1402.6907 [hep-ph].
- [28] A. Bazavov *et al.*, Phys. Rev. D **88**, 094021 (2013), arXiv:1309.2317 [hep-lat].
- [29] E. Follana *et al.* (HPQCD Collaboration, UKQCD Collaboration), Phys. Rev. D **75**, 054502 (2007), arXiv:hep-lat/0610092 [hep-lat].
- [30] A. Bazavov *et al.*, Phys. Rev. D **85**, 054503 (2012), arXiv:1111.1710 [hep-lat].
- [31] A. Bazavov *et al.* (HotQCD), Phys. Rev. **D90**, 094503 (2014), arXiv:1407.6387 [hep-lat].
- [32] M. Clark, A. Kennedy, and Z. Sroczynski, Nucl. Phys. Proc. Suppl. **140**, 835 (2005), arXiv:hep-lat/0409133 [hep-lat].
- [33] C. Allton *et al.*, Phys. Rev. D **66**, 074507 (2002), arXiv:hep-lat/0204010 [hep-lat].
- [34] <http://www.rproject.org/>, .
- [35] P. Hegde, F. Karsch, E. Laermann, and S. Shcheredin, Eur. Phys. J. **C55**, 423 (2008), arXiv:0801.4883 [hep-lat].
- [36] E. Braaten and A. Nieto, Phys. Rev. D **53**, 3421 (1996), arXiv:hep-ph/9510408 [hep-ph].
- [37] K. Kajantie, M. Laine, K. Rummukainen, and M. E. Shaposhnikov, Nucl. Phys. B **503**, 357 (1997), arXiv:hep-ph/9704416 [hep-ph].
- [38] M. Laine and Y. Schroder, Journal of High Energy Phys. **03**, 067 (2005), arXiv:hep-ph/0503061 [hep-ph].
- [39] R. Bellwied, S. Borsanyi, Z. Fodor, S. D. Katz, A. Pasztor, C. Ratti, and K. K. Szabo, (2015), arXiv:1507.04627 [hep-lat].